

# On Ultrahigh-energy Neutrino Scattering

**Masaaki Kuroda**

Institute of Physics, Meijigakuin University  
Yokohama, Japan

**Dieter Schildknecht**

Fakultät für Physik, Universität Bielefeld  
D-33501 Bielefeld, Germany

and

Max-Planck Institute für Physik (Werner-Heisenberg-Institut),  
Föhringer Ring 6, D-80805, München, Germany

## Abstract

We predict the neutrino-nucleon cross section at ultrahigh energies relevant in connection with the search for high-energy cosmic neutrinos. Our investigation, employing the color-dipole picture, among other things allows us to quantitatively determine which fraction of the ultrahigh-energy neutrino-nucleon cross section stems from the saturation versus the color-transparency region. We disagree with various results in the literature that predict a strong suppression of the neutrino-nucleon cross section at neutrino energies above  $E \cong 10^9 GeV$ . Suppression in the sense of a diminished increase of the neutrino-nucleon cross section with energy only starts to occur at neutrino energies beyond  $E \cong 10^{14} GeV$ .

Initiated by the experimental search for cosmic neutrinos of energies larger than  $E \simeq 10^6 \text{GeV}^1$ , the theoretical investigation<sup>2</sup> of the neutrino-nucleon interaction at ultrahigh energies received much attention recently. Predictions require a considerable extension of the theory of neutrino-nucleon deep inelastic scattering (DIS) into a kinematic domain beyond the one where results from experimental tests are available at present. Different theoretical approaches have been employed ranging from conventional linear evolution of nucleon parton distributions to the investigation of possible non-linear effects conjectured to becoming relevant in the ultrahigh-energy domain.

In the present note, we consider neutrino scattering in the framework of the color dipole picture (CDP)<sup>3</sup>. The CDP is uniquely suited for a treatment of ultrahigh-energy neutrino scattering. Extrapolating the results from electron-proton scattering at HERA, we expect the total neutrino-nucleon cross section at ultrahigh energies to be dominantly due to the kinematic range of  $x \ll 0.1$  of the Bjorken variable  $x_{bj} \equiv x \cong Q^2/W^2$ . This is the domain of validity of the CDP.

In particular, we shall focus on the question of color transparency versus saturation. Does the total neutrino-nucleon cross section at ultrahigh energies dominantly originate from the region of large values of the low-x scaling variable [4, 5],

$$\eta(W^2, Q^2) = \frac{(Q^2 + m_0^2)}{\Lambda_{sat}^2(W^2)}, \quad (1)$$

namely  $\eta(W^2, Q^2) \gg 1$  (“color transparency” region), or is there a substantial part that is due to the kinematic range of  $\eta(W^2, Q^2) \ll 1$  (“saturation” region)?

In (1),  $\Lambda_{sat}^2(W^2)$  denotes the “saturation scale” that increases with the  $\gamma^*(Z^0, W^\pm)p$  center-of-mass energy squared,  $W^2$ , as  $(W^2)^{C_2}$ , where  $C_2 \simeq 0.29$  (compare (12) below). At HERA energies,  $\Lambda_{sat}^2(W^2)$  approximately ranges from  $2\text{GeV}^2 \lesssim \Lambda_{sat}^2(W^2) \lesssim 7\text{GeV}^2$ . The  $\gamma^*(Z^0, W^\pm)$  virtual four-momenta squared in (1) is denoted by  $q^2 = -Q^2$ , and  $m_0^2 \simeq 0.15\text{GeV}^2$  (for light quarks). Compare Fig. 1 for the  $(Q^2, W^2)$  plane with the line of  $\eta(W^2, Q^2) = 1$ .

---

<sup>1</sup>Compare refs. 16-24 in [1]

<sup>2</sup>Compare e.g. refs. 2-8 in [2]

<sup>3</sup>Compare ref. [3] for recent reviews on the CDP and an extensive list of references.

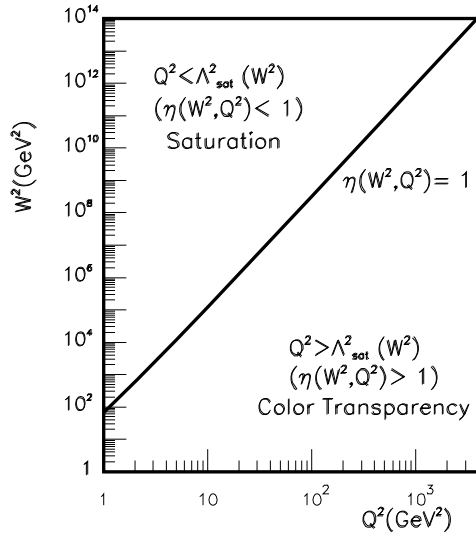


Figure 1: The  $(Q^2, W^2)$  plane showing the line  $\eta(W^2, Q^2) = 1$  that separates the saturation region from the color-transparency region.

The charged-current neutrino-nucleon cross section we shall concentrate on, as a function of the neutrino energy,  $E$ , is given by (e.g. [6])

$$\sigma_{\nu N}(E) = \int_{Q_{min}^2}^s dQ^2 \int_{\frac{Q^2}{s}}^1 dx \frac{1}{xs} \frac{\partial^2 \sigma}{\partial x \partial y}, \quad (2)$$

where

$$\frac{\partial^2 \sigma}{\partial x \partial y} = G_F^2 \frac{s}{2\pi} \left( \frac{M_W^2}{Q^2 + M_W^2} \right)^2 \sigma_r(x, Q^2), \quad (3)$$

and  $\sigma_r(x, Q^2)$  in (3) denotes the “reduced cross section”

$$\sigma_r(x, Q^2) = \frac{1 + (1 - y)^2}{2} F_2^\nu(x, Q^2) - \frac{y^2}{2} F_L^\nu(x, Q^2) + y(1 - \frac{y}{2}) x F_3^\nu(x, Q^2). \quad (4)$$

In standard notation,  $s$  denotes the neutrino-nucleon center-of-mass energy squared,

$$s = 2M_p E + M_p^2 \cong 2M_p E, \quad (5)$$

with  $M_p$  being the nucleon mass,  $q^2 = -Q^2$  is the four-momentum squared transferred from the neutrino to the  $W^\pm$  boson of mass  $M_W$ , and  $G_F$  is the Fermi coupling. The Bjorken variable is given by

$$x = \frac{Q^2}{2qP} = \frac{Q^2}{W^2 + Q^2 - M_p^2} \cong \frac{Q^2}{W^2}, \quad (6)$$

where the approximate equality in (6) is valid in the relevant range of  $x \ll 0.1$ . The fraction of the energy transfer from the neutrino to the  $W^\pm$  boson,  $y$ , is given by

$$y = \frac{Q^2}{2M_p E x} \cong \frac{W^2}{s}. \quad (7)$$

For the subsequent discussion, it will be useful to replace the integration over  $dx$  in (2) by an integration over  $W^2$ , rewriting (2) as

$$\sigma_{\nu N}(E) = \frac{G_F^2}{2\pi} \int_{Q_{min.}^2}^{s-M_p^2} dQ^2 \left( \frac{M_W^2}{Q^2 + M_W^2} \right)^2 \int_{M_p^2}^{s-Q^2} \frac{dW^2}{W^2} \sigma_r(x, Q^2). \quad (8)$$

Due to the vector-boson propagator, contributions to the total cross section for  $Q^2 \gg M_W^2$  are strongly suppressed, and with  $W^2 \leq s$  and  $s$  in the ultrahigh energy range,  $s \gg M_W^2$ , we expect the cross section to dominantly originate from  $x \approx Q^2/W^2 \ll 0.1$ .

In what follows, we concentrate on the (dominant) contribution due to  $F_2^\nu(x, Q^2)$  in (8) according to (4).<sup>4</sup>

For small values of  $x \lesssim 0.1$ , DIS of electrons and neutrinos on nucleons, in terms of, respectively, the  $\gamma^*p$  and the  $(W^\pm, Z^0)p$  forward scattering amplitude, proceeds via scattering of long-lived massive hadronic fluctuations,  $\gamma^*(Z^0) \rightarrow q\bar{q}$  and  $W^- \rightarrow \bar{u}d$  etc., that undergo diffractive forward scattering on the nucleon (CDP) [3].

For the flavor-symmetric  $(q\bar{q})N$  interaction at  $x \ll 0.1$ , the neutrino-nucleon structure function,  $F_2^{\nu N}(x, Q^2)$ , and the electromagnetic structure function,  $F_2^{eN}(x, Q^2)$ , are related by  $(1/n_f)F_2^{\nu N}(x, Q^2) = (1/\sum_q Q_q^2)F_2^{eN}(x, Q^2)$ , or

$$F_{2,L}^{\nu N}(x, Q^2) = \frac{n_f}{\sum_q^{n_f} Q_q^2} F_{2,L}^{eN}(x, Q^2), \quad (9)$$

where  $n_f$  denotes the number of actively contributing quark flavors, and  $Q_q$  the quark charge, and  $n_f/\sum_q Q_q^2 = 18/5$  for  $n_f = 4$  flavors of quarks. As a consequence of the proportionality (9), the total neutrino-nucleon cross section (8) may be predicted by inserting the electromagnetic structure function into (4).

The electromagnetic structure function,  $F_2^{ep}(x, Q^2)$ , is related to the total

---

<sup>4</sup>The contribution due to  $F_L^\nu(x, Q^2)$  turned out to be less than 6 %, compare the discussion in connection with Table 4 below. The contribution from the structure function  $F_3(x, Q^2)$  in (4), that is due to valence-quark interactions, can be ignored.

photoabsorption cross section,  $\sigma_{\gamma^*p}(W^2, Q^2)$ , by<sup>5</sup>

$$F_2^{ep}(x, Q^2) = \frac{Q^2}{4\pi^2\alpha} \sigma_{\gamma^*p}(W^2, Q^2). \quad (10)$$

In the CDP, as a consequence [4, 7] of the interaction of the color dipole with the gluon field in the nucleon, the photoabsorption cross section becomes a function of the low- $x$  scaling variable,  $\eta(W^2, Q^2)$ ,

$$\sigma_{\gamma^*p}(W^2, Q^2) = \sigma_{\gamma^*p}(\eta(W^2, Q^2)) \sim \sigma^{(\infty)} \begin{cases} \ln \frac{1}{\eta(W^2, Q^2)} & , \text{ for } \eta(W^2, Q^2) \ll 1, \\ \frac{1}{2\eta(W^2, Q^2)} & , \text{ for } \eta(W^2, Q^2) \gg 1, \end{cases} \quad (11)$$

where the cross section  $\sigma^{(\infty)} \equiv \sigma^{(\infty)}(W^2)$  is of hadronic size, and, at most, it depends weakly on  $W^2$ . Both, the dependence on the single variable  $\eta(W^2, Q^2)$  (for  $\sigma^{(\infty)} \cong \text{const.}$ ) in (11), and the specific functional form of this dependence, are general consequences [4, 7] of the color-gauge-invariant interaction of a  $(q\bar{q})$  dipole with the color field in the nucleon. Any specific ansatz for a parameterization of the dipole-nucleon cross section has to provide an interpolation between the  $\ln(1/\eta(W^2, Q^2))$  and the  $1/2\eta(W^2, Q^2)$  dependence in (11). It is well known [4], compare Fig. 2, that the depen-

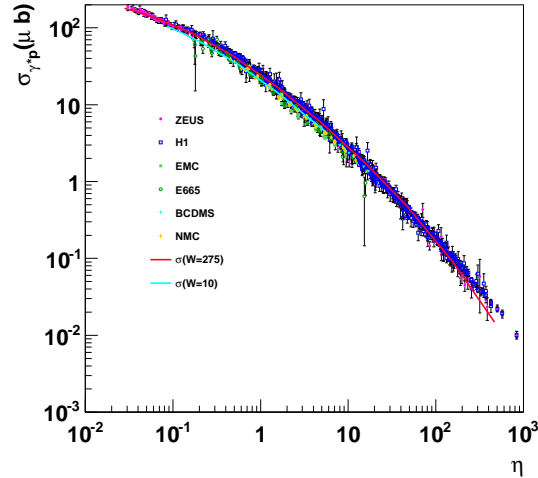


Figure 2: The theoretical prediction [4, 7] for the photoabsorption cross section  $\sigma_{\gamma^*p}(\eta(W^2, Q^2))$  compared with the experimental data on DIS.

dence (11) on the single variable  $\eta(W^2, Q^2)$  is fulfilled by the experimental data with  $\sigma^{(\infty)} \cong \text{const.}$  in the HERA energy range. The saturation scale is

<sup>5</sup>The low- $x$  approximation is used for the factor in front of  $\sigma_{\gamma^*p}(W^2, Q^2)$  in (10).

given by [4, 5, 7]

$$\Lambda_{sat}^2(W^2) = C_1 \left( \frac{W^2}{1\text{GeV}^2} \right)^{C_2}, \quad C_1 = 0.34 \text{ GeV}^2, \quad C_2 \cong 0.29. \quad (12)$$

The value of the exponent  $C_2 \cong 0.29$  is fixed [7] by requiring consistency of the CDP with the pQCD-improved parton model.

We return to neutrino scattering. Employing relation (9), we replace the neutrino structure function,  $F_2^\nu(x, Q^2)$ , in (4) by the electromagnetic one,  $F_2^{ep}(x, Q^2)$ , or rather by the photoabsorption cross section, compare (10). The neutrino-nucleon total cross section (8) becomes<sup>6</sup>

$$\begin{aligned} \sigma_{\nu N}(E) &= \frac{G_F^2 M_W^4}{8\pi^3 \alpha} \sum_q \frac{n_f}{Q_q^2} \int_{Q_{Min}^2}^{s-M_p^2} dQ^2 \frac{Q^2}{(Q^2 + M_W^2)^2} \\ &\times \int_{M_p^2}^{s-Q^2} \frac{dW^2}{W^2} \frac{1}{2} (1 + (1-y)^2) \sigma_{\gamma^* p}(\eta(W^2, Q^2)). \end{aligned} \quad (13)$$

We first of all look at the ratio

$$r(E) = \frac{\sigma_{\nu N}(E)_{\eta(W^2, Q^2) < 1}}{\sigma_{\nu N}(E)}. \quad (14)$$

In (14),  $\sigma_{\nu N}(E)_{\eta(W^2, Q^2) < 1}$  denotes that part of the total neutrino-nucleon cross section in (13) that originates from contributions from the saturation region of  $\eta(W^2, Q^2) < 1$  in Fig. 1. This part of the total cross section (13) is obtained by imposing the cut of  $\eta(W^2, Q^2) < 1$  on the  $(Q^2, W^2)$  integration domain in (13). According to (1) and (12), the restriction of  $\eta(W^2, Q^2) < 1$  (for  $Q_{Max}^2 \geq Q^2 \geq Q_{Min}^2 = \Lambda_{sat}^2(M_p^2) - m_0^2$ , and  $Q_{Max}^2 \gg m_0^2$ ) upon employing  $W_{Max}^2 = s - Q^2$ , yields

$$\begin{aligned} W^2 \geq W^2(Q^2)_{Min} &= \left( \frac{Q^2 + m_0^2}{C_1} \right)^{\frac{1}{C_2}}, \\ Q^2 \leq Q_{Max}^2 &= \Lambda_{sat}^2(s) \left( 1 - C_2 \frac{\Lambda_{sat}^2(s)}{s} + o\left(\frac{\Lambda_{sat}^4(s)}{s^2}\right) \right). \end{aligned} \quad (15)$$

From (15), for the ultrahigh-energy corresponding to  $s = 10^{14} \text{ GeV}^2$ , with (12), one finds  $Q^2 < Q_{Max}^2 = \Lambda_{sat}^2(s) = 3.9 \times 10^3 \text{ GeV}^2 \ll s$ . We observe that even for  $s = 10^{14} \text{ GeV}^2$ , the range of  $Q^2 < Q_{Max}^2$  covered under restriction (15) is smaller than the  $W^\pm$  mass squared,  $M_W^2 \approx 6.4 \times 10^3 \text{ GeV}^2$ , that determines the maximum of the  $Q^2$ -dependent factor in (13). We accordingly expect a small value of  $r(E) \ll 1$ .

---

<sup>6</sup>We restrict ourselves to the dominant term  $F_2^\nu(x, Q^2)$  in (4), ignoring  $F_L(x, Q^2)$  and  $F_3(x, Q^2)$ .

The ratio  $r(E)$  in (14) is evaluated in two steps. In a first step, we only rely on the very general low- $x$  scaling restrictions for  $\sigma_{\gamma^*p}(\eta(W^2, Q^2))$  in (11) with (12) and derive an upper bound on  $r(E) < \bar{r}(E)$  on  $r(E)$ . In a second step, we introduce a concrete representation for  $\sigma_{\gamma^*p}(\eta(W^2, Q^2))$  in the CDP that smoothly interpolates the regions of  $\eta(W^2, Q^2) < 1$  and  $\eta(W^2, Q^2) > 1$  in (11).

The ratio  $r(E)$  in (14), upon substituting (13) and taking into account (15), becomes

$$r(E) = \frac{\int_{Q_{Min}^2}^{Q_{Max}^2(s)} dQ^2 \frac{Q^2}{(Q^2 + M_W^2)^2} \int_{W^2(Q^2)_{Min}}^{s-Q^2} \frac{dW^2}{W^2} (1 + (1-y)^2) \sigma_{\gamma^*p}(\eta(W^2, Q^2))}{\int_{Q_{Min}^2}^{s-M_p^2} dQ^2 \frac{Q^2}{(Q^2 + M_W^2)^2} \int_{M_p^2}^{s-Q^2} \frac{dW^2}{W^2} (1 + (1-y)^2) \sigma_{\gamma^*p}(\eta(W^2, Q^2))}. \quad (16)$$

Using the scaling behaviour (11) for  $\eta(W^2, Q^2) < 1$  and  $\eta(W^2, Q^2) > 1$ , we derive an upper limit,

$$r(E) < \bar{r}(E), \quad (17)$$

on the ratio  $r(E)$  in (16). Appropriately substituting the behaviour (11) of  $\sigma_{\gamma^*p}(\eta(W^2, Q^2))$  into (16), and simplifying by putting  $y = 0$  in the numerator and  $y = 1$  in the denominator, an upper bound on  $r(E)$  reads<sup>7</sup>

$$\bar{r}(E) = \frac{2 \int_{Q_{Min}^2}^{Q_{Max}^2(s)} dQ^2 \frac{Q^2}{(Q^2 + M_W^2)^2} \int_{W^2(Q^2)_{Min}}^{s-Q^2} \frac{dW^2}{W^2} \ln \frac{1}{\eta(W^2, Q^2)}}{\int_{Q_{Min}^2}^{s-M_p^2} dQ^2 \frac{Q^2}{(Q^2 + M_W^2)^2} \int_{M_p^2}^{s-Q^2} \frac{dW^2}{W^2} \frac{1}{2\eta(W^2, Q^2)}}. \quad (18)$$

For  $\Lambda_{sat}^2(s) < M_W^2 \ll s$ , one finds that the numerator in (18) is approximately given by

$$N(E) = \frac{1}{2} \frac{1}{2C_2} \left( \frac{\Lambda_{sat}^2(s)}{M_W^2} \right)^2 + o\left( \left( \frac{\Lambda_{sat}^2(s)}{M_W^2} \right)^3 \right). \quad (19)$$

The denominator in (18) becomes

$$D(E) = \frac{1}{2C_2} \left( \frac{\Lambda_{sat}^2(s)}{M_W^2} \right) \left( 1 + o\left( \frac{M_W^2}{s} \log \frac{M_W^2}{s} \right) \right). \quad (20)$$

Inserting (19) and (20) into (18), we find the upper bound on  $r(E)$ ,

$$r(E) < \bar{r}(E) = \frac{1}{2} \frac{\Lambda_{sat}^2(s)}{M_W^2}. \quad (21)$$

Numerical values of  $\bar{r}(E)$ , using (12), are given in Table 1, together with the results for  $r(E)$  resulting from an explicit expression for  $\sigma_{\gamma^*p}(\eta(W^2, Q^2))$  from the CDP to be discussed below.

<sup>7</sup>In the denominator of (18), we inserted the  $1/2\eta(W^2, Q^2)$  dependence only valid for  $\eta(W^2, Q^2) > 1$ . We explicitly checked that the enlargement of the cross section as a consequence of this approximation amounts to only a few percent in the energy range up to  $E \sim 10^{14}$  GeV under consideration.

$E(\text{GeV})$	$\bar{r}(E)$	$r(E) _{\text{Table3}}$	$r(E) _{\text{Table4}}$
$10^6$	$1.74 \times 10^{-3}$	$1.40 \times 10^{-3}$	$4.58 \times 10^{-3}$
$10^{10}$	$2.51 \times 10^{-2}$	$1.63 \times 10^{-2}$	$2.55 \times 10^{-2}$
$10^{14}$	$3.63 \times 10^{-1}$	$1.76 \times 10^{-1}$	$1.96 \times 10^{-1}$

Table 1: The upper bound,  $\bar{r}(E) > r(E)$ , on the fraction of the total neutrino-nucleon cross section originating from the saturation region of  $\eta(W^2, Q^2) < 1$ . The results for  $\bar{r}(E)$  in the second column are based on (21) with (12). The results for  $r(E)|_{\text{Table 3}}$  are based on evaluating (16) upon substitution of (22) with (25). The results for  $r(E)|_{\text{Table 4}}$  are based on evaluating (16) upon substitution of (29) with (25).

According to (21) and Table 1, the fraction of the total neutrino-nucleon cross section arising from the saturation region is strongly suppressed. The saturation region contributes less than a few percent, except for extremely ultrahigh energies of order  $E \simeq 10^{14}\text{GeV}$ .

We turn to an evaluation of the neutrino-nucleon cross section based on an explicit form of  $\sigma_{\gamma^*p}(\eta(W^2, Q^2))$  in the CDP.

The CDP leads to a remarkably simple form of the photoabsorption cross section that moreover can be represented by a closed expression,<sup>8</sup> [4, 7]

$$\begin{aligned} \sigma_{\gamma^*p}(W^2, Q^2) &= \sigma_{\gamma^*p}(\eta(W^2, Q^2)) + O\left(\frac{m_0^2}{\Lambda_{\text{sat}}^2(W^2)}\right) = \\ &= \frac{\alpha R_{e^+e^-}}{3\pi} \sigma^{(\infty)}(W^2) I_0(\eta(W^2, Q^2)) + O\left(\frac{m_0^2}{\Lambda_{\text{sat}}^2(W^2)}\right), \end{aligned} \quad (22)$$

where

$$\begin{aligned} I_0(\eta(W^2, Q^2)) &= \frac{1}{\sqrt{1+4\eta(W^2, Q^2)}} \ln \frac{\sqrt{1+4\eta(W^2, Q^2)}+1}{\sqrt{1+4\eta(W^2, Q^2)}-1} \cong \\ &\cong \begin{cases} \ln \frac{1}{\eta(W^2, Q^2)} + O(\eta \ln \eta), & \text{for } \eta(W^2, Q^2) \rightarrow \frac{m_0^2}{\Lambda_{\text{sat}}^2(W^2)}, \\ \frac{1}{2\eta(W^2, Q^2)} + O\left(\frac{1}{\eta^2}\right), & \text{for } \eta(W^2, Q^2) \rightarrow \infty, \end{cases} \end{aligned} \quad (23)$$

and

$$R_{e^+e^-} = 3 \sum_q Q_q^2. \quad (24)$$

Comparing (22) and (23) with (11), one notes that (22) smoothly interpolates the regions of  $\eta(W^2, Q^2) \ll 1$  and  $\eta(W^2, Q^2) \gg 1$  in (11).

---

<sup>8</sup>We note that the closed form for the photoabsorption cross section in (22) with (23) contains the simplifying assumption of ‘‘helicity independence’’ leading to  $F_L^{ep} = 0.33 F_2^{ep}$  rather than  $F_L^{ep} = 0.27 F_2^{ep}$ . This simplifying approximation is unimportant in the present context. Compare refs. [7, 8] for the refinement that implies the result  $F_L^{ep} = 0.27 F_2^{ep}$  that is consistent with the HERA experimental observations.

The (weak) energy dependence of the dipole cross section  $\sigma^{(\infty)}(W^2)$  in (22) is determined by consistency of  $\sigma_{\gamma^*p}(W^2, Q^2)$  with Regge behavior [4, 9] in the photoproduction limit of  $\sigma_{\gamma p}(W^2) = \sigma_{\gamma^*p}(W^2, Q^2 = 0)$ , and alternatively, by consistency with the double-logarithmic fit to photoproduction by the Particle Data Group,

$$\sigma^{(\infty)}(W^2) = \frac{3\pi}{R_{e^+e^-} \alpha} \frac{1}{\ln \frac{\Lambda_{sat}^2(W^2)}{m_0^2}} \begin{cases} \sigma_{\gamma p}^{Regge}(W^2), \\ \sigma_{\gamma p}^{PDG}(W^2). \end{cases} \quad (25)$$

The fits to photoproduction, compare refs. [4], [9] and [10] (in units of  $mb$ , with  $W^2$  in  $\text{GeV}^2$ ) are explicitly given by

$$\begin{aligned} \sigma_{\gamma p}^{(a)}(W^2) &= 0.0635(W^2)^{0.097} + 0.145(W^2)^{-0.5}, \\ \sigma_{\gamma p}^{(b)}(W^2) &= 0.0677(W^2)^{0.0808} + 0.129(W^2)^{-0.4525} \\ \sigma_{\gamma p}^{(c)}(W^2) &= 0.003056 \left( 33.71 + \frac{\pi}{M^2} \ln^2 \frac{W^2}{(M_p + M)^2} \right) \\ &\quad + 0.0128 \left( \frac{(M_p + M)^2}{W^2} \right)^{0.462}, \end{aligned} \quad (26)$$

where  $M_p$  stands for the proton mass and  $M = 2.15\text{GeV}$ . Concerning the energy dependence of the photoabsorption cross section in (22), we note that the growth  $\sigma_{\gamma^*p}(W^2, Q^2) \sim (\ln W^2)(W^2)^{C_2}$  in the color-transparency region (for  $\sigma^{(\infty)}(W^2) \sim \sigma_{\gamma p}^{PDG}(W^2)/\ln \frac{\Lambda_{sat}^2(W^2)}{m_0^2}$ ) of  $\eta(W^2, Q^2) > 1$  turns into the slower growth of  $\sigma_{\gamma^*p}(W^2, Q^2) \sim (\ln W^2)^2$ , once the saturation limit of  $\eta(W^2, Q^2) < 1$  is reached.

In Table 2, we present the results for the neutrino-nucleon cross section based on (13)<sup>9</sup> upon substitution of the photoabsorption cross section from (22) with  $\Lambda_{sat}^2(W^2)$  from (12),  $m_0^2 = 0.15\text{GeV}^2$ , and  $\sigma^{(\infty)}(W^2)$  determined by (25) and (26). The results in Table 2 for  $\sigma_{\nu N}^{(b)}(E)$  and  $\sigma_{\nu N}^{(c)}(E)$  based on  $\sigma^{(\infty)}(W^2)$  from the Regge fit (b) and the PDG fit (c), respectively, coincide in good approximation. The enhancement of the cross section  $\sigma_{\nu N}^{(a)}(E)$  relative to  $\sigma_{\nu N}^{(b,c)}(E)$  is a consequence of the stronger increase of the Pomeron contribution ( $(W^2)^{0.097}$  versus  $(W^2)^{0.0808}$ ) in  $\sigma^{(\infty)}(W^2)$  originating from (26). At the highest energy under consideration,  $E = 10^{14}\text{GeV}$ , the enhancement reaches

---

<sup>9</sup>The CDP contains the limit of  $Q^2 \rightarrow 0$ , such that  $Q_{Min}^2$  may be put to  $Q_{Min}^2 = 0$  in (13). The actual dependence on  $Q_{Min}^2$  is negligible, as long as  $0 \lesssim Q_{Min}^2 \lesssim M_p^2$ . We also note tht the replacement of the lower limit  $W^2 \geq M_p^2$  by  $W^2 \geq \text{const } M_p^2$  for e.g.  $\text{const} \leq 20$  leads to an insignificant change of the neutrino cross section.

$E$	1.0E+04	1.0E+06	1.0E+08	1.0E+10	1.0E+12	1.0E+14
$\sigma_{\nu N}^{(a)}$	1.28E-34	1.91E-33	1.09E-32	5.36E-32	2.60E-31	1.23E-30
$\sigma_{\nu N}^{(b)}$	1.21E-34	1.68E-33	8.96E-33	4.11E-32	1.85E-31	8.15E-31
$\sigma_{\nu N}^{(c)}$	1.19E-34	1.69E-33	9.26E-33	4.29E-32	1.88E-31	7.77E-31

Table 2: The prediction of the neutrino-nucleon cross section,  $\sigma_{\nu N}^{(a,b,c)}[cm^2]$ , from the CDP as a function of the neutrino energy,  $E[GeV]$ . Compare text for details.

a factor of about 1.5. Concerning the energy dependence, by comparing neighboring results in Table 2 for  $E \geq 10^8 GeV$ , one notes an increase (only) slightly stronger than expected from the proportionality to  $\Lambda_{sat}^2(s) \sim s^{C_2}$  in the estimate (20). This is a consequence of the energy dependence (25) of  $\sigma^{(\infty)} = \sigma^{(\infty)}(W^2)$  ignored in (20).

We return to the question of the relative contribution to the neutrino cross section from the saturation region relative to the color-transparency region. We subdivide the neutrino cross section into the sum

$$\sigma_{\nu N}^{(c)}(E) = \sigma_{\nu N}^{(c)}(E)_{\eta(W^2, Q^2) < 1} + \sigma_{\nu N}^{(c)}(E)_{\eta(W^2, Q^2) > 1}. \quad (27)$$

The results are shown in Table 3. From Table 3, one finds that the fraction

$E$	1.0E+04	1.0E+06	1.0E+08	1.0E+10	1.0E+12	1.0E+14
$\sigma_{\nu N}^{(c)}$	1.19E-34	1.69E-33	9.26E-33	4.29E-32	1.88E-31	7.77E-31
$\eta > 1$	1.19E-34	1.68E-33	9.22E-33	4.22E-32	1.77E-31	6.41E-31
$\eta < 1$	1.14E-37	2.37E-36	4.15E-35	6.97E-34	1.08E-32	1.37E-31

Table 3: The contributions to the neutrino-nucleon cross section  $\sigma_{\nu N}^{(c)}(E)$  [ $cm^2$ ] as a function of  $E[GeV]$  from the color transparency ( $\eta(W^2, Q^2) > 1$ ) and the saturation ( $\eta(W^2, Q^2) < 1$ ) region compared with the full cross section,  $\sigma_{\nu N}^{(c)}(E)$  taken from Table 2.

of the total cross section originating from the saturation region,  $r(E)$  in (14) and (16), increases from  $r(E = 10^6 GeV)|_{Table3} \cong 1.40 \cdot 10^{-3}$  to  $r(E = 10^{14} GeV)|_{Table3} \cong 1.76 \cdot 10^{-1}$ . The increase is consistent with the upper bound (21), compare Table 1. With increasing energy, there is a strong increase from the saturation region, but even at  $E = 10^{14} GeV$  its contribution is of the order of only 17%.

The result that the dominant part of the neutrino-nucleon cross section is due to contributions from large values of  $\eta(W^2, Q^2) \gg 1$  requires further examination. For e.g. a value of  $Q^2 = 10^4 GeV^2 \cong M_W^2$ , and for  $W^2$  below

$W^2 \leq 10^5 \text{GeV}^2$  (or  $x \leq 0.1$ ), one finds that  $\eta(W^2, Q^2)$  reaches values of  $\eta(W^2, Q^2) \leq \eta_{Max}(W^2, Q^2) \cong 10^3$ . For such large values of  $\eta(W^2, Q^2)$ , as previously analysed [4, 7], the theoretical expression (22) for the photoabsorption cross section must be corrected by elimination of contributions from high-mass ( $q\bar{q}$ ) fluctuations,  $\gamma^* \rightarrow q\bar{q}$ , of mass  $M_{q\bar{q}}$ . The life time of high-mass fluctuations in the rest frame of the nucleon becomes too short to be able to actively contribute to the  $q\bar{q}$ -color-dipole interaction. The restriction on the  $q\bar{q}$  mass,  $m_0^2 \leq M_{q\bar{q}}^2 \leq m_1^2(W^2)$  is taken care of by the energy-dependent upper bound,  $m_1^2(W^2)$ , where

$$m_1^2(W^2) = \xi \Lambda_{sat}^2(W^2), \quad (28)$$

and empirically  $\xi = 130$  [7]. Employing the restriction (28) extends the validity of the CDP to high values of  $\eta(W^2, Q^2) \gg 1$ .

Explicitly, one finds that (22) must be modified by a factor that depends on the ratio of  $\xi/\eta(W^2, Q^2)$ . One obtains [7]

$$\begin{aligned} \sigma_{\gamma^*p}(W^2, Q^2) &= \frac{\alpha R_{e^+e^-} \sigma^{(\infty)}(W^2) I_0(\eta(W^2, Q^2))}{3\pi} \\ &\times \frac{1}{3} \left( G_L \left( \frac{\xi}{\eta(W^2, Q^2)} \right) + 2G_T \left( \frac{\xi}{\eta(W^2, Q^2)} \right) \right) \\ &+ O \left( \frac{m_0^2}{\Lambda_{sat}^2(W^2)} \right) \end{aligned} \quad (29)$$

where

$$\begin{aligned} &\frac{1}{3} \left( G_L \left( \frac{\xi}{\eta(W^2, Q^2)} \right) + 2G_T \left( \frac{\xi}{\eta(W^2, Q^2)} \right) \right) = \\ &\frac{1}{\left( 1 + \frac{\xi}{\eta(W^2, Q^2)} \right)^3} \left( \left( \frac{\xi}{\eta(W^2, Q^2)} \right)^3 + 2 \left( \frac{\xi}{\eta(W^2, Q^2)} \right)^2 + \left( \frac{\xi}{\eta(W^2, Q^2)} \right) \right) \\ &\cong \begin{cases} 1 & , \text{ for } \eta(W^2, Q^2) \ll \xi = 130 \\ \frac{\xi}{\eta(W^2, Q^2)} & , \text{ for } \eta(W^2, Q^2) \gg \xi = 130 \end{cases} ; \end{aligned} \quad (30)$$

We note in passing that the theoretical prediction shown in Fig. 2 includes[7] the large- $\eta(W^2, Q^2)$  correction (29)<sup>10</sup>.

In Table 4, third and fourth line, we present our final results for the neutrino-nucleon cross section based on substituting (29) into (13). The

---

<sup>10</sup>The photoabsorption cross section obtained from the simple closed expression (29) coincides within a (negative) deviation of up to approximately 25 % with the results shown in fig. 2 that are based on the more elaborate treatment in ref.[7], compare footnote 8

E	1.0E+04	1.0E+06	1.0E+08	1.0E+10	1.0E+12	1.0E+14
$\sigma_{\nu N}^{(c)}$	1.19E-34	1.69E-33	9.26E-33	4.29E-32	1.88E-31	7.77E-31
	3.85E-35	5.15E-34	4.17E-33	2.73E-32	1.49E-31	6.96E-31
	3.19E-35	3.80E-34	2.83E-33	1.75E-32	9.12E-32	4.11E-31

Table 4: The neutrino-nucleon cross section,  $\sigma_{\nu N}^{(c)}(E)[cm^2]$ , as a function of the neutrino energy  $E[GeV]$  upon imposing the restriction (28) on the mass of actively contributing  $q\bar{q}$  fluctuations (3rd and 4th line) compared with the result from Table 3 (2nd line) that ignores the restriction (28). The results in the 3rd and 4th line are based on  $\Lambda_{sat}^2(W^2) \sim (W^2)^{C_2}$  with  $C_2 = 0.29$  and  $C_2 = 0.27$ , respectively.

PDG result for  $\sigma^{(\infty)}(W^2)$  in (25) is used, and, for comparison, the result for  $\sigma_{\nu N}^{(c)}(E)$  from Table 2 ( i.e.  $\sigma_{\nu N}^{(c)}(E)$  without the restriction (28)) is again shown in the second line of Table 4. We explicitly verified that the addition in (13) of the contribution corresponding to the longitudinal structure function according to (4) diminishes the neutrino cross section in Table 4 by less than 6 % in the whole range of neutrino energies under consideration. In order to demonstrate the sensitivity under variation of the exponent  $C_2$  of the energy dependence of the saturation scale,  $\Lambda_{sat}^2(W^2) \sim (W^2)^{C_2}$ , in Table 4, we give the neutrino-nucleon cross section for  $C_2 = 0.29$  and  $C_2 = 0.27$ . Both values are consistent with the available experimental information on DIS.

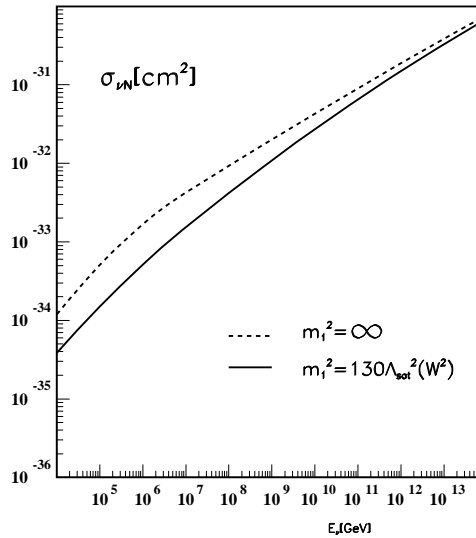


Figure 3: The effect on the neutrino-nucleon cross section of excluding inactive high-mass  $q\bar{q}$  fluctuations.

The results from Table 4 (2nd and 3rd line) are graphically represented

in Fig. 3. With increasing neutrino energy, the exclusion of inactive large-mass  $q\bar{q}$  fluctuations by the restriction of  $M_{q\bar{q}}^2 < m_1^2(W^2) = \xi\Lambda_{sat}^2(W^2)$ , where  $\xi = 130$ , becomes less important. Most of the contributions to the neutrino-nucleon cross section in the extreme ultrahigh-energy limit ( $E \simeq 10^{14}$  GeV) are due to moderately large values of  $\eta(W^2, Q^2)$  that correspond to  $q\bar{q}$  fluctuations of sufficiently long life time. Quantitatively, from Table 4, at  $E = 10^4$  GeV the cross section is diminished by a factor of 0.32, while at  $E = 10^{14}$  GeV, this factor is equal to 0.89. This effect is also seen in the ratio  $r(E)$  in Table 1. At  $E = 10^6$  GeV, the ratio  $r(E)$  exceeds the crude estimate of  $\bar{r}(E)$  from (18).

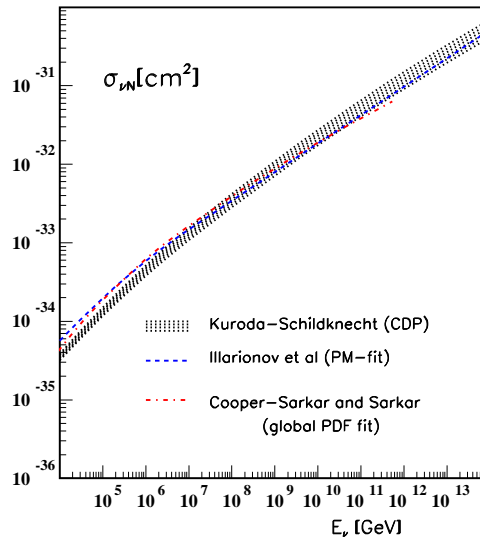


Figure 4: Comparison of the CDP prediction for the neutrino-nucleon cross section,  $\sigma_{\nu N}(E)[cm^2]$ , according to (13) with (29) and  $\sigma_{\gamma p}^{PDG}(W^2)$  from (25), with the predictions from the pQCD-improved parton model. The band of the prediction from the CDP illustrates the sensitivity of  $\sigma_{\nu N}(E)$  under variation of the exponent  $C_2$  in  $\Lambda_{sat}^2(W^2) \sim (W^2)^{C_2}$  between  $C_2 = 0.27$  and  $C_2 = 0.29$ .

In Fig. 4, we compare our final results for the neutrino-nucleon cross section,  $\sigma_{\nu N}(E) \equiv \sigma_{\nu N}^{(c)}(E)$  from Table 4, 3rd and 4th line, based on the CDP, with the ones obtained [1, 2] by employing the parton distributions from a conventional perturbative QCD (pQCD) analysis of DIS. Fig. 4 shows consistency of our CDP results with the ones from the pQCD-improved parton model. Our predictions are also consistent with the ones in ref. [11].

A series of recent papers [12] - [15] treats DIS at HERA energies and ultra-high-energy neutrino scattering by adopting an ansatz with an  $(\ln W^2)^2$  dependence of the underlying hadron-nucleon cross section. The ansatz is based on the asymptotic behavior of strong-interaction cross sections as  $(\ln W^2)^2$  due to Heisenberg[16] and Froissart[17].

The ansatz of  $F_2^{ep}(x, Q^2) \sim \sum_{n,m=0,1,2} a_{nm}(\ln Q^2)^n(\ln(1/x))^m$ , with seven free fit parameters [12] - [15], yields a successful representation of the HERA experimental results for all  $x$  and  $Q^2$  in the region of  $x \lesssim 0.1$ . The subsequent evaluation [12] - [15] of the neutrino-nucleon cross section with this ansatz for  $F_2^{ep}(x, Q^2)$ , essentially according to (9) and (13), for  $E \gtrsim 10^9 GeV$  led to a cross section that is suppressed relative to pQCD results, and, consequently, also in comparison with our CDP predictions. Compare Fig. 5.

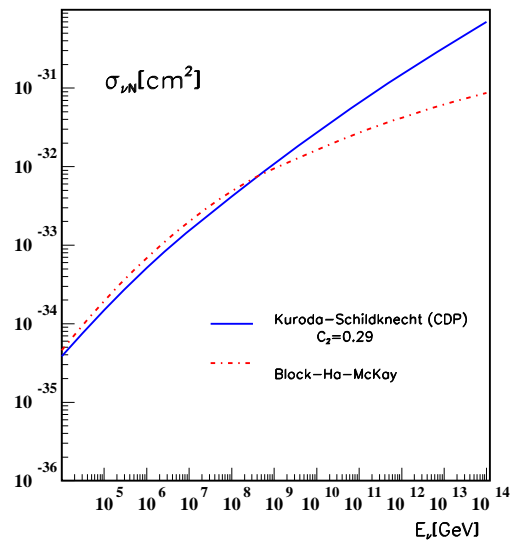


Figure 5: A comparison of the results for the neutrino-nucleon cross section from the CDP according to fig. 4 with the results from the “Froissart-inspired” ansatz from [14].

Since the CDP contains an  $(\ln W^2)^2$  dependence, compare e.g. the discussion immediately following (26), the result of Fig. 5 may look like an inconsistency. The apparent inconsistency is resolved in fig. 6. Figure 6 shows the prediction for the neutrino-nucleon cross section from the CDP for an extended energy range up to  $E = 10^{24} GeV$ . As seen in fig. 6, in consistency with the  $(\ln W^2)^2$  dependence of  $\sigma_{\gamma^*p}(W^2, Q^2)$  in the saturation region of  $\eta(W^2, Q^2) < 1$ , also the CDP implies a decreasing growth of the

neutrino-nucleon cross section. In distinction from the prediction from the “Froissart-inspired” ansatz, the decreasing growth of the cross section in the CDP is shifted to energies above  $E \cong 10^{14} GeV$ .

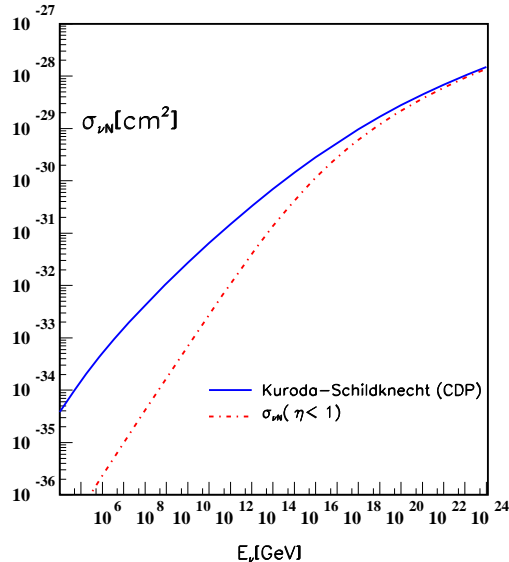


Figure 6: The neutrino-nucleon total cross section,  $\sigma_{\nu N}(E) \equiv \sigma_{\nu N}^{(c)}(E)$ , from the CDP as a function of the neutrino energy  $E$  for the extended range of energies up to  $E = 10^{24} GeV$ . For comparison, we also show that part of the cross section,  $\sigma_{\nu N}(E)|_{\eta(W^2, Q^2) < 1}$ , that is obtained upon restricting the contributions of  $\sigma_{\gamma^* p}(W^2, Q^2)$  to the neutrino-nucleon cross section to the saturation region of  $\eta(W^2, Q^2) < 1$ .

In Fig. 6, we explicitly demonstrate that the reduced growth of the neutrino cross section with increasing energy is directly connected with the increasingly smaller contribution due to  $\sigma_{\nu N}^{(c)}(E)_{\eta(W^2, Q^2) > 1}$  in (27). In the ultra-ultra-high-energy limit, the neutrino-nucleon cross section in (13) becomes saturated by contributions from that region of the photoabsorption cross section where the  $(\ln(W^2))^2$  dependence becomes dominant.

We must conclude that the requirement of a “Froissart-like” ansatz for the underlying hadron-nucleon cross section *by itself does not* imply a weaker growth, compared with e.g. the pQCD prediction, for the neutrino-nucleon cross section above  $E = 10^9 GeV$ . It is the combination of the energy dependence for  $F_2^{ep}(x, Q^2)$ , contained in  $\ln(1/x)$  and  $(\ln(1/x))^2$  terms, with the seven-free-parameter fit to the ad hoc polynomial  $\ln Q^2$  dependence of the coefficients of the  $\ln(1/x)$  and  $(\ln(1/x))^2$  terms that leads to a suppression above  $E = 10^9 GeV$ .

In the CDP, the  $Q^2$  dependence is uniquely fixed by the  $Q^2$  dependence of the “photon-wave function”, i.e. the transition of the (virtual) photon to  $q\bar{q}$  dipole states with subsequent propagation of these  $q\bar{q}$  states of mass  $M_{q\bar{q}}$ . The interaction of the  $q\bar{q}$  color dipoles is restricted by being a gauge-invariant interaction with the gluon field in the nucleon.

Taking into account the more detailed dynamics of the CDP, and the much smaller number of free fit parameters, compared with the  $\ln(1/x)$  and  $(\ln(1/x))^2$  ansatz, we are thus led to disagree with the conclusion of an onset of a suppression of the neutrino-nucleon cross section for  $E \gtrsim 10^9 GeV$  implied by the analysis [12] - [15] of the “Froissart-inspired” ansatz.

A suppression, in the sense of a reduced growth of the total neutrino-nucleon cross section with increasing energy, is expected to occur, however, for neutrino energies beyond  $E = 10^{14} GeV$ .

## Acknowledgement

Questions on the subject matter by Paolo Castorina and by participants of the Oberwoelz symposium on Quantum Chromodynamics, History and Prospects (Oberwoelz, Austria, September 3 – 8, 2012) are gratefully acknowledged.

## References

- [1] A. Cooper-Sarkar and S. Sarkar, JHEP **01** (2008) 075.
- [2] A.Yu. Illarionov, B.A. Kniehl and A.V. Kotikov, Phys. Rev. Lett. **106** (2011) 231802;  
M.M. Block, P. Ha, D.W. McKay, arXiv: 1110.6665v1 [hep-ph].
- [3] D. Schildknecht, Invited Talk, Ringberg Workshop on New Trends in HERA Physics, Ringberg Castle, September 25-28,2011, Nucl. Phys. B, Proc. Supplement **222-224** (2012) 108;  
D. Schildknecht, Invited Talk, 50th International School of Subnuclear Physics, Erice, Italy, June 23 – July 2, 2012, arXiv: 1210.0733v1 [hep-ph], to appear in the Proceedings, ed. by A. Zichichi (World Scientific);  
D. Schildknecht, to appear in Proceedings of Diffraction 2012 (Amer-

ican Institute of Physics, A. Papa, editor), Lanzarote, Canary Islands (Spain), September 10-15,2012, arXiv: 1301.0714v1 [hep-ph].

- [4] D. Schildknecht, in Diffraction 2000, Cetraro, Italy, September 2-7, 2000, Nucl. Phys. B, Proc. Supplement **99** (2001) 121;  
D. Schildknecht, B. Surrow, M. Tentyukov, Phys. Lett. **B499** (2001) 116;  
G. Cvetic, D. Schildknecht, B. Surrow, M. Tentyukov, EPJC **20** (2001) 77.
- [5] D. Schildknecht, Contribution to DIS 2001, The 9th International Workshop on Deep Inelastic Scattering, Bologna, Italy, 2001, G. Brassi et al. (Eds.), World Scientific, Singapore, 2002, p. 798;  
D. Schildknecht, B. Surrow and M. Tentyukov, Mod. Phys. Lett. **A16** (2001) 1829.
- [6] V.P. Gonçalves and P. Hepp, Phys. Rev **D83** (2011) 014014.
- [7] M. Kuroda and D. Schildknecht, Phys. Rev. **D85** (2012) 094001.
- [8] M. Kuroda and D. Schildknecht, Phys. Lett. **B670** (2008) 129;  
D. Schildknecht, Phys. Lett.**B716** (2012) 413.
- [9] S. Donnachie and P. Landshoff, Phys. Lett. **B296** (1992) 227.
- [10] Particle Data Group, Phys. Rev. **D86** (2012) 1.
- [11] R. Fiore, L.L. Jenkovszky, A.V. Kotikov, F. Paccanoni, A. Papa and E. Predazzi, Phys. Rev. **D68** (2003) 093010;  
R. Fiore, L.L. Jenkovszky, A.V. Kotikov, F. Paccanoni and A. Papa, Phys. Rev. **D73** (2006) 053012.
- [12] M.M. Block, E. Berger and C.-I. Tan, Phys. Rev. Lett. **97** (2006) 252003;  
E. Berger, M. Block and C.-I. Tan, Phys. Rev. Lett. **98** (2007) 242001.
- [13] E. Berger, M.M. Block, D. McKay and C.-I. Tan, Phys. Rev. **D77** (2008) 053007.
- [14] M.M. Block, P. Ha and D. McKay, Phys. Rev. **D82** (2010) 077302.

- [15] M.M. Block, L. Durand, P. Ha, D.W. McKay, arXiv: 1302.6119v2 [hep-ph]  
M.M. Block, L. Durand, P. Ha, D.W. McKay, arXiv: 1302.6172v1 [hep-ph]
- [16] W. Heisenberg, Vorträge über kosmische Strahlung (Springer, Berlin,1953), p.155, reprinted in W. Heisenberg, Collected Works, Series B, p.498 (Springer, Berlin,1984);  
Die Naturwissenschaften 61 (1974) 1, reprinted in Collected Works, Series B, p.912.
- [17] M. Froissart, Phys. Rev. **123** (1961) 1053.